Solution properties of xanthan. Light scattering and viscometry on dilute and moderately concentrated solutions

Takakazu Kojima* and G. C. Berry†
Carnegie-Mellon University, Department of Chemistry, 4400 Fifth Avenue, Pittsburgh, PA 15213, USA
(Received 15 January 1988; accepted 18 April 1988)

Elastic and quasi-elastic light-scattering, viscometric and rheological studies are given for solutions of the microbial polysaccharide *Xanthomonas campestris* (xanthan) in aqueous 0.62 N NaCl for polymer concentrations from 0.03 to 2.2 g kg^{-1}. The observed negative $\partial \ln[\eta]/\partial \ln T$ is interpreted as a decrease of the persistence length with increasing T. The behaviour in moderately concentrated solutions ($2 < [\eta]c < 25$) reveals intermolecular association, leading to gel formation in the extreme case. The effect of the association on the viscometric and light-scattering data is discussed. It is concluded that the early stages of association involve structure with the chain axes nearly parallel, but that larger, particulate-like structures develop with increasing c, eventually leading to gel formation under certain conditions.

(Keywords: xanthan; association; persistence length; light scattering; viscometry; gel)

INTRODUCTION

Light-scattering, viscometric and rheological studies are presented in the following for solutions of the microbial polysaccharide *Xanthomonas campestris* (xanthan) in aqueous 0.62 N NaCl. The light-scattering data include both elastic and quasi-elastic measurements. Taken together, the solutions studied span the concentration range 0.03 to 2.2 g kg^{-1} and temperatures from 25 to 80°C. Dilute-solution parameters are obtained at the lower end of the concentration range, and gel formation was observed for the highest concentration studied. The behaviour in dilute solutions is discussed in terms of a temperature-dependent persistence length for xanthan, and that at intermediate concentration is represented in terms of microgel components in an otherwise fluid-like solution.

EXPERIMENTAL

Materials

The sample of xanthan used in this study was supplied as an aqueous stock solution by G. F. Hardy, Celanese Research Co., Summit, NJ. The sample was prepared from the fermentation broth of the bacterium *Xanthomonas campestris* NRRL B-1459 by a process of sequential filtrations. The broth was heated to 100°C, slurried with diatomaceous earth, diluted to about 3 g kg^{-1} and filtered to remove all debris, etc., to obtain a clarified dilute solution of xanthan. The latter was then increased in concentration to 21.7 g kg^{-1} by ultrafiltration. The solution was analysed to have 1.2 g kg^{-1} pyruvic acid, 8.9 g kg^{-1} carbon and 3.7 g kg^{-1} ash comprising 40% K, 5% P, 3% Na, 3% Ca, 2% Mg and 1% Si, with smaller concentrations of other metals. The pyruvic acid concentration corresponds to 64% pyruvate substitution on the xanthan. The excess of potassium indicates that the xanthan is largely in the form of the potassium salt.

Solutions used here were prepared by dilution of the stock solution with aqueous 0.62 N NaCl containing 0.003 N sodium azide. After dilution to about three times the final concentration desired, the solution was stirred at room temperature for 48 h, then at 80°C for 2 h, and lightly sonicated for 6 h at room temperature. The solution was then diluted to the desired level and the preceding repeated. The final dilution was filtered through a membrane filter (0.3 μm pore size). For light-scattering studies the solution was filtered directly into a light-scattering cell suitable for subsequent centrifugation. The solution was then degassed by freeze–thaw cycles and finally flame-sealed in the container under vacuum.

The preceding procedure was not followed in one case for a solution prepared for rheological studies of a xanthan gel. In that case the stock solution was centrifuged for 1.5 h at 1500 g, and then diluted to form the solution studied.

Light scattering

The light-scattering method, apparatus, data acquisition system and correlator are described in detail elsewhere[1]. The vertically polarized 514.5 nm line of an argon-ion laser was used as the incident beam.

The photon-count correlation function $g^{(2)}(\tau, q)$ was determined as[1]:

$$g^{(2)}(\tau, q) = G^{(2)}(\tau, q)/\langle n \rangle_q^2 \quad (1)$$

$$G^{(2)}(\tau, q) = \frac{1}{M} \sum_{j=1}^{M} \frac{1}{T} \left(\sum_{i=1}^{T} n_i n_{i+k} \right)_j \quad (2)$$

* Present address: National Defense Academy, Yokosuka, Japan
† To whom correspondence should be addressed

0032-3861/88/122249-12$03.00

Table 1 Viscometric data for aqueous xanthan solution[a] (0.62 N NaCl)

	$T=70°C$		$T=25°C$	
w (g kg^{-1})	η_{rel}	$[\eta]_c$ (ml g^{-1})	η_{rel}	$[\eta]_c$ (ml g^{-1})
0.0325	1.226	6640	1.4102	11190
0.0654	–	–	1.8732	10680
0.1670	2.321	5990	–	–
0.1875	–	–	4.7289	11090
0.2511	–	–	7.1632	11500
0.3164	3.709	5410	–	–
0.374	–	–	14.290	12290
0.434	5.383	5480	–	–
0.515	–	–	28.397	13430
0.585	10.04	6420	–	–
0.757	17.03	6940	–	–
0.930	25.24	7130	84.219	13460
1.250	133	13050	580	27000

[a] $[\eta]_c$ is defined by equation (6)

where $\tau=k\,\Delta\tau$, with k an integer and $\Delta\tau$ the sampling interval equal to $(50\times10^{-9})2^N$ s, with N adjustable from 6 to 24, $\langle n\rangle$ is the average count rate, $T=2^{12}$, M was adjusted so that the total number of counts $\langle n\rangle TM$ was about 10^6, and $q=(4\pi n/\lambda)\sin(\theta/2)$, with θ the scattering angle, λ the wavelength of the incident beam in vacuum and n the solution refractive index. In most experiments, k was from 1 to 32, but in some cases the upper bound was increased to 64. Values of $\Delta\tau$ were chosen in successive experiments to permit evaluation of any curvature in $\ln[g^{(2)}(\tau,q)-1]$ *versus* τ over the range for $g^{(2)}(\tau,q)-1$ greater than about 0.001.

The average count rate $\langle n\rangle$ was used to compute the Rayleigh ratio R as $k_\lambda\langle n\rangle/\langle n\rangle_{std}$ where $\langle n\rangle_{std}$ is the count rate from a working standard comprising a polystyrene solution in a cell similar to that used for the solutions studied and k_λ is equal to $(4\pi^2/N_A\lambda^4)k^*$, where k^* is independent of λ (k^* is equal to 13.0 for the arrangement used).

Viscometry

Filtered solution prepared as described above was used in a Couette viscometer described elsewhere[2]. The instrument was sealed to prevent loss of solvent by evaporation, and constructed so that only glass surfaces contact the test solution. The outer cylinder (radius R_2) is stationary and a torque imposed on the inner cylinder (radius R_1) causes it to rotate with rotational velocity Ω. The inner cylinder is held in the centre of the outer cylinder through the effects of surface tension at the meniscus formed between the two cylinders, following a design of Zimm and Crothers[3]. An aluminium cylinder is placed inside the inner glass cylinder so that a torque L may be generated by the action of a magnetic field rotating at angular velocity Ω_M, with $L\propto\Omega_M-\Omega$. With this instrument, the relative viscosity η_{rel} may be determined by measurement of $P=2\pi/\Omega$ for the solution, and $P_0=2\pi/\Omega_0$ for the solvent, with[2]:

$$\eta_{rel}=(P-P_M)/(P_0-P_M) \tag{3}$$

where $P_M=2\pi/\Omega_M$; values of P_M/s equal to 1, 6 and 30 were used. The average shear rate κ is given by:

$$\kappa=(\pi/P)[(R_2+R_1)/(R_2-R_1)]f(R_1,R_2) \tag{4}$$

where $f(R_1,R_2)$ is nearly unity for the values $R_1=9$ mm and $R_2=11$ mm used here, so that $\kappa\approx10\pi/P$. Since $P-P_M=P_MK_L\eta/d$, with d the density and K_L a constant ($K_L\approx120$ in cgs units for the instrument used here), values of P, and hence κ, varied with η and P_M such that:

$$\kappa=10\pi/P_M(1+K_L\eta/d) \tag{5}$$

The shear stress σ may be calculated as $K_S(\Omega_M-\Omega)$ where K_S is a constant ($K_S\approx0.26$ in cgs units for the instrument used here). Thus, σ is less than $2\pi K_S/P_M$, which would be the stress if the inner cylinder did not rotate (as would be the case, for example, with a gel under constant L).

Rheological measurements

The rheological properties of a sample that proved to be a gel were examined using a cone-and-plate rheometer described elsewhere[4]. A concentric glass ring around the cone and plate served to suppress evaporation of water from the gel. Rheological measurements were made about 4 h after the sample was installed in the rheometer. Creep and recovery were done with a shear stress of 0.07 Pa, and dynamic mechanical experiments were performed with a stress amplitude of 0.44 Pa.

RESULTS

Viscometry

The viscometric data given in *Table 1* are shown as $[\eta]_c$ vs. c in *Figure 1* for $c<1$ g l^{-1}, where $\eta_{sp}=\eta_{rel}-1$ and:

$$[\eta]_c=(1/c)[2(\eta_{sp}-\ln\eta_{rel})]^{1/2} \tag{6}$$

These data were obtained with the concentric-cylinder viscometer described above, with shear rates given by equation (5). For dilute solutions, the usual relations:

$$\eta_{sp}/c=[\eta]\{1+k'[\eta]c+k''([\eta]c)^2+\cdots\} \tag{7}$$

$$\ln\eta_{rel}/c=[\eta]\{1-(\tfrac{1}{2}-k')[\eta]c+(\tfrac{1}{3}-k'+k'')([\eta]c)^2+\cdots\} \tag{8}$$

result on the assumption of a Taylor series expansion of η_{rel} in powers of c. With these expressions:

$$[\eta]_c=[\eta]\{1-(\tfrac{1}{3}-k')[\eta]c+\cdots\} \tag{9}$$

so that $[\eta]_c\approx[\eta]$ if $k'\approx1/3$, as is frequently the case for polymer solutions under conditions with $T>\Theta$, where Θ is the temperature for which the second virial coefficient vanishes. The data in *Figure 1* give $[\eta]$/ml g^{-1} equal to 11300 and 6800 and k' equal to 0.34 and 0.23 for T equal to 25 and 70°C, respectively. As seen in *Figure 1*, $[\eta]_c\approx[\eta]$ for $c<0.4$ g l^{-1}.

A generalization of equation (7) in the form[5,6]:

$$\eta_{sp}/[\eta]c=P(K_Mk'[\eta]c) \tag{10}$$

where $P(0)$ is unity is sometimes useful to correlate data

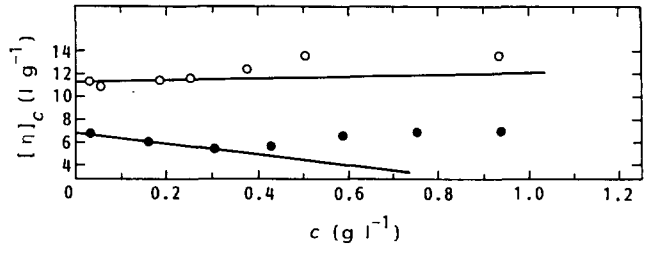

Figure 1 The function $[\eta]_c=c^{-1}[2(\eta_{sp}-\ln\eta_{rel})]^{1/2}$ *versus* c for solutions of xanthan in aqueous 0.62 N NaCl at 25°C (○) and 70°C (●)

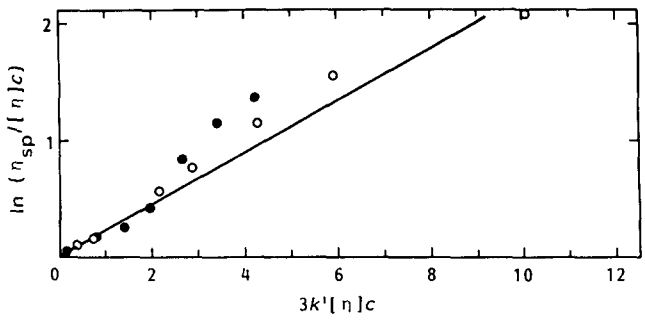

Figure 2 The function $\ln(\eta_{sp}/[\eta]c)$ *versus* $3k'[\eta]c$ for solutions of xanthan in aqueous 0.62 N NaCl; symbols as in *Figure 1*. The full line represents equations (10) and (11) with $K_M = 0.74$

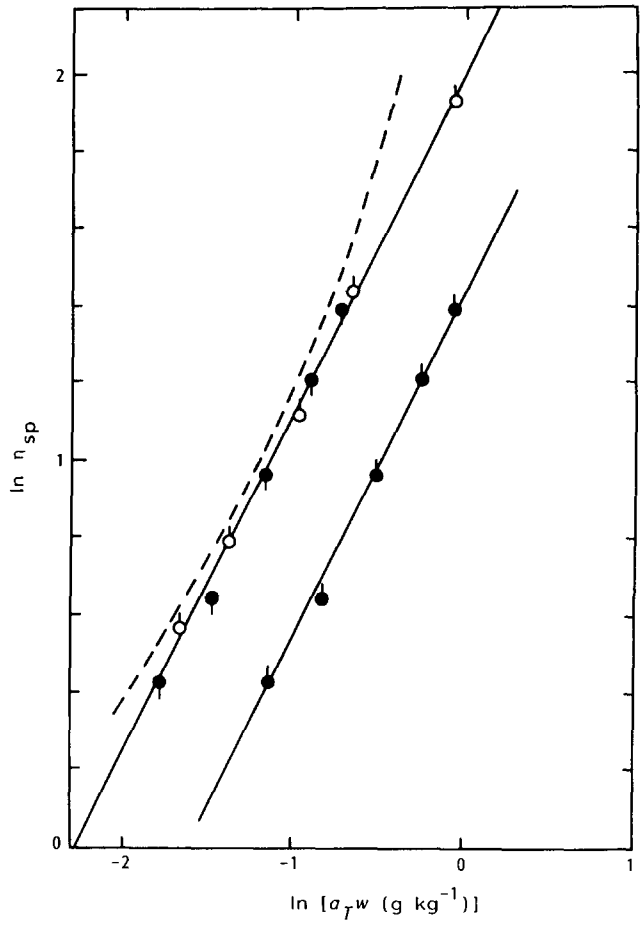

Figure 3 A plot of $\log \eta_{sp}$ *versus* $\log(a_T w/\text{g kg}^{-1})$ for solutions of xanthan in aqueous 0.62 N NaCl at 25°C (○) and 70°C (●), with $a_T = 1$ (pips up) or a_T given by equations (12) (pips down). The broken curve represents equation (10), with $P(0.44[\eta]c)$ given by equation (13), following results in ref. 8

on η_{sp} as a function of c for the range of $[\eta]c$ of interest here. For example, in one commonly used relation[7]:

$$P(x) = \exp x \tag{11}$$

Use of equations (10) and (11) with $K_M = 1$ will produce equations (7) and (8) to order $([\eta]c)^2$, with $k'' = (k')^2/2$. As shown in *Figure 2*, equations (10) and (11) provide an approximate correlation for the data obtained here for $[\eta]c < 2$, with $K_M = 0.74$, which is similar to values of K_M reported for polystyrene in a variety of solvents[5]. With increasing $[\eta]c$, the viscosities are underestimated by equations (10) and (11) using the K_M found for $[\eta]c < 2$, but as shown in *Figure 3* for $[\eta]c > 2$ the data obtained for w up to 0.93 g kg^{-1} obey a power-law relation of the form $\eta_{sp} = (a_T w)^{\mu}$, where $\mu = 2.05$ and:

$$a_T = \left(\frac{\eta_{sp}(T)}{\eta_{sp}(T_R)}\right)^{1/\mu} \tag{12}$$

Also shown in *Figure 3* is a correlation reported[8] for solutions of 'native' xanthan and samples prepared therefrom by ultrasonic degradation. That correlation represents η_{sp} by equation (10) with:

$$P(x) = 1 + x + 0.25x^{3.24} \tag{13}$$

where $K_M k' = 0.44$. In terms of equation (10) the power-law behaviour shown in *Figure 3* gives $P = K_M(k'[\eta]c)^{\mu - 1}$ for $[\eta]c > 2$, with $K_M = 2.12$ for T equal to 25 or 70°C, and:

$$a_T^{\mu} = \frac{\{(k'[\eta]\rho)^{\mu-1}[\eta]\rho\}_T}{\{(k'[\eta]\rho)^{\mu-1}[\eta]\rho\}_{T_R}} \tag{14}$$

with $T_R = 25$°C, or $a_T = 0.48$ for $T = 70$°C. Thus, it appears that $\eta_{sp}/[\eta]c$ scales with the parameters k' and $[\eta]$ found at infinite dilution, even though the form of P is complex, and both k' and $[\eta]$ depend on T. The plot of $\ln \eta_{sp}$ vs. T^{-1} in *Figure 4* for a solution with $w = 0.93$ g kg^{-1} gives $W = \partial \ln \eta_{sp}/\partial T^{-1} = 2550$K. By comparison, W is 1800K for water. Since the data on $\ln \eta_{sp}$ vs. $\ln a_T w$ superpose for $w > 0.3$ g kg^{-1}, and $\eta_{sp} \propto w^{\mu}$ in this range, a_T may be expressed as

$$\ln a_T = (T^{-1} - T_R^{-1})W/\mu \tag{15}$$

where T_R is an (arbitrary) reference temperature, equal to 25°C here.

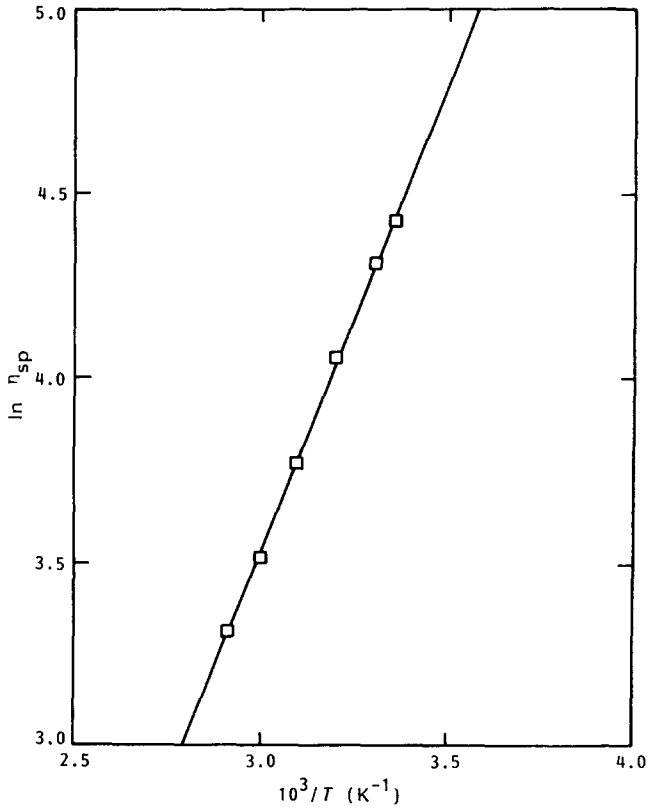

Figure 4 A plot of $\ln \eta_{sp}$ *versus* T^{-1} for a solution of xanthan in 0.62 N NaCl with $w = 0.93$ g kg^{-1}

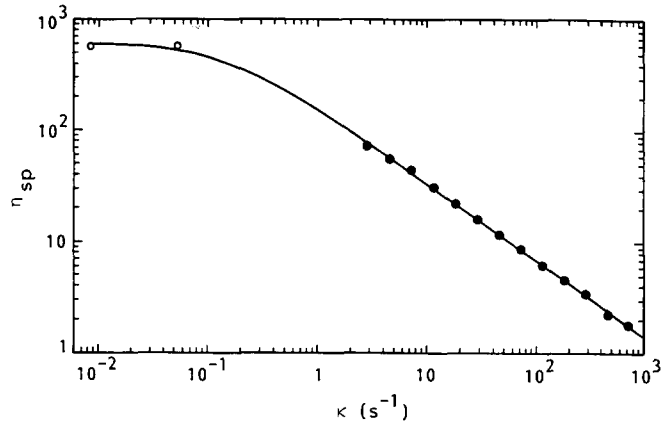

Figure 5 A plot of $\log \eta_{sp}$ *versus* κ/s^{-1} for a solution of xanthan in 0.62 N NaCl with $w = 1.25\,g\,kg^{-1}$. The data were obtained with a couette (○) or cone-and-plate (●) instruments, as discussed in the text. The full curve represents $\eta_{sp}(\kappa)/\eta_{sp}(0)$ *versus* $\tau_c\kappa$ for a typical polymer fluid[9], scaled to give $\eta_{sp}(0)$ at low κ, and with $\tau_c = 7.85$ s

In the preceding, all viscosities are reported for experiments at low shear rate κ. Data on the steady-state viscosity η_κ as a function of κ are shown in *Figure 5* for a solution with $w = 1.25\,g\,kg^{-1}$. For many polymer solutions, η_κ obeys a relation of the form[9]:

$$\eta_\kappa = \eta_0 F(\tau_c\kappa) \tag{16}$$

where η_0 is the limiting value of η_κ for small κ, $F(0) = 1$ and τ_c is a time constant equal to $R_0^{(s)}\eta_0$, with $R_0^{(s)}$ the linear steady-state recoverable compliances (sometimes referred to as J_e^0). For many systems, $F(1) \approx 0.7$. The data on η_{sp} as a function of κ are shown in comparison with a curve computed with $F(\tau_c\kappa)$ for a typical polymer fluid[9], using $\tau_c = 7.85$ s, or $R_0^{(s)} = 12.6\,Pa^{-1}$. These results verify that the data reported in *Table 1* represent limiting viscosities at low shear rate.

Viscoelasticity

An unfiltered solution with $w = 2.2\,g\,kg^{-1}$ was observed to form a gel at 25°C. The properties of this gel are shown in *Figure 6* giving the linear recoverable compliance $R(t)$, the storage compliance $J'(\omega)$ and the dynamic viscosity $\eta'(\omega)$ calculated as $G''(\omega)/\omega = J''(\omega)/\omega[J^{(D)}(\omega)]^2$, where $G''(\omega)$ and $J''(\omega)$ are the loss modulus and compliance, respectively, and[9,10]:

$$[J^{(D)}(\omega)]^2 = [J'(\omega)]^2 + [J''(\omega)]^2 \tag{17}$$

The recoverable compliance was computed from the recoverable strain following creep under a stress of 0.07 Pa for a duration long enough that the final rate of creep was essentially zero. Under these conditions, the creep compliance $J(t)$ was found to be equal to $R(t)$, showing the sample to be a viscoelastic solid. A stress amplitude of 0.44 Pa was used in measurements of $\eta'(\omega)$ and $J'(\omega)$.

These results show that a gel was obtained, with an equilibrium modulus G_e of about 6 Pa, and an 'internal viscosity' given by the limit of $\eta'(\omega)$ for small ω of about 360 Pa s. By comparison, the viscosity obtained by use of equation (10) with equation (13) for $P(x)$ is 13 Pa s. If it is assumed that the relaxation modulus has the form:

$$G(t) = G_e + [G(0) - G_e]\sum g_i \exp(-t/\tau_i) \tag{18}$$

where the τ_i are the viscoelastic relaxation times, and the weighting factors g_i are so normalized that $\sum g_i = 1$, then[9]:

$$\eta'(\omega) = [G(0) - G_e]\sum_i \frac{g_i\tau_i}{1+(\omega\tau_i)^2} \tag{19}$$

$$J'(\omega) = R(0) + [G_e^{-1} - R(0)]\sum_i \frac{h_i}{1+(\omega\lambda_i)^2} \tag{20}$$

$$R(t) = G_e^{-1} - [G_e^{-1} - R(0)]\sum_i h_i \exp(-t/\lambda_i) \tag{21}$$

where the λ_i are retardation times, and the weight factors h_i are so normalized that $\sum h_i = 1$. For the solid, the relation[9,10]:

$$\int_0^t G(u)R(t-u)\,du = t \tag{22}$$

provides a connection between the set of parameters for the h_i and λ_i and that for the g_i and τ_i. The data in *Figure 5* can be represented by equations (18) to (22) with τ_i ranging from 0.1 ms to 70 s, with the latter representing the time constant for the approach of $G(t)$ to G_e for large t.

Light scattering

The scattered intensity is shown as a function of $\sin^2(\theta/2)$ in *Figure 7* for two of the solutions of xanthan prepared as described above and centrifuged for 30 min using a swinging bucket rotor, with a centrifugal field of about 7000*g*. The two solutions span the concentration range studied by light scattering. In both cases, the data exhibit enhanced scattering at small angles (see below). A scaling length b defined as:

$$b^2 = -3\lim_{q=0}[\partial \ln R(q)/\partial q^2] \tag{23}$$

with $R(q)$ the Rayleigh ratio, is about equal to 150 nm, being relatively independent of temperature and concentration. (In the simplest case at infinite dilution, b^2 is the mean-square radius of gyration of the chain[11,12].) The constancy in $qR(q)$ observed for $\theta > 60°$ is discussed below.

Several variables affect the data on $g^{(2)}(\tau, q)$ including: the temperature, the duration of centrifugation prior to

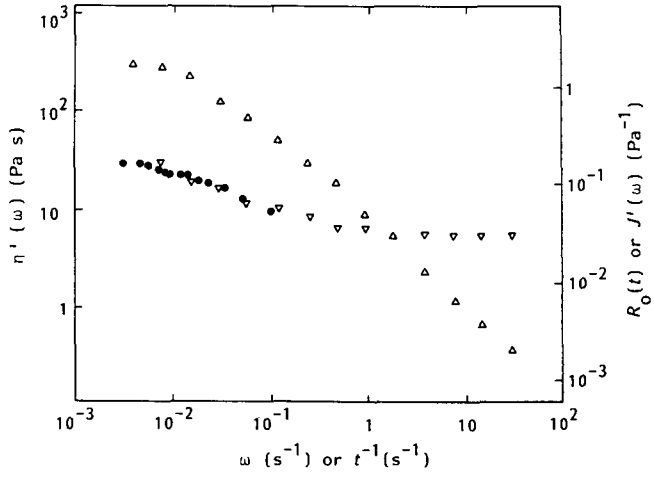

Figure 6 Rheological data for a gel of xanthan in 0.62 N NaCl with $w = 2.2\,g\,kg^{-1}$ showing the recoverable shear compliance $R_0(t)$ (●) as a function of t^{-1}, the storage shear compliance $J'(\omega)$ (▽) and the dynamic viscosity $\eta'(\omega)$ (△) as a function of ω

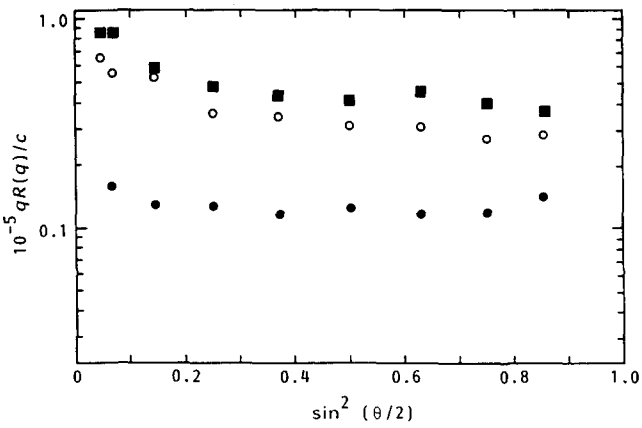

Figure 7 Plots of $\log qR(q)/c$ *versus* $\sin^2(\theta/2)$ for solutions of xanthan in 0.62 N NaCl with w/g kg^{-1} equal to 0.19 (○, ■) or 2.2 (●) at 25°C (circles) or 79°C (squares)

the light-scattering measurement, and the position of the scattering volume in the light-scattering cell (i.e. the position in the centrifugal field prior to the scattering experiment). Scattering data reported here are confined to the concentration range $0.19 < w/\text{g kg}^{-1} < 2.20$. In all cases, the data could be represented in the form[12]:

$$g^{(2)}(\tau, q) - 1 = [g^{(2)}(0, q) - 1][\sum r_\nu \exp(-\gamma_\nu \tau)]^2 \quad (24)$$

where $\sum r_\nu = 1$. The factor $g^{(2)}(0, q) - 1$ depends on the sample geometry. Methods described elsewhere[12,13] were used to compute r_ν and γ_ν for the few (3–4) terms needed to fit equation (24) to experimental data (see below). Although the fundamental significance of the r_ν and γ_ν so obtained may be open to question, they at least permit a means to represent experimental results in condensed form, and quantify differences among $g^{(2)}(\tau, q)$ for a series of similar materials. The relation:

$$g^{(2)}(\tau, q) - 1 = [g^{(2)}(0, q) - 1]\exp[-(\gamma\tau)^n] \quad (25)$$

sometimes found to represent non-exponential behaviour[14,15], does not fit the data obtained in this study.

In representing the γ_ν, it is convenient to reduce all data by multiplication of γ_ν^{-1} by the factors a_θ and $a_{\eta_s}^{-1}$, given by:

$$a_\theta = \left(\frac{\sin(\theta/2)}{\sin(\theta_R/2)}\right)^2 \quad (26)$$

$$a_{\eta_s}^{-1} = \frac{T\eta_s(T_R)}{T_R\eta_s(T)} \quad (27)$$

with a reference scattering angle θ_R of 30° and a reference temperature T_R of 25°C, where $\eta_s(T)$ is the solvent viscosity at temperature T. Thus, for a simple case, $a_\theta a_{\eta_s}^{-1}\gamma_\nu^{-1}$ would be independent of both θ and T (see below).

The effects of centrifugation and temperature are illustrated in *Figure 8*. Values of the corresponding r_ν and $a_\theta a_{\eta_s}^{-1}\gamma_\nu^{-1}$ given in *Tables 2* and *3* may be used to reconstruct the $g^{(2)}(\tau, q)$ shown in *Figure 8* along with $g^{(2)}(\tau, q)$ obtained in additional experiments. Four conditions are represented in *Figure 8*, depending on the duration t_{cent} of centrifugation of the light-scattering cell in a swinging bucket rotor at 30°C (angular velocity $\omega \approx 830$ rad s^{-1} and centrifugal field of $\sim 7000g$), and the subsequent temperature T_{LS} of the sample for the light-scattering experiment: (a) $t_{cent} = 0.5$ h, $T_{LS} = 25$°C; (b) $t_{cent} = 0.5$ h, $T_{LS} = 78$°C; (c) $t_{cent} = 12$ h, $T_{LS} = 25$°C; (d) $t_{cent} = 12$ h, $T_{LS} = 78$°C. As seen in *Figure 8*, in every case plots of $g^{(2)}(\tau, q)$ *versus* $a_\theta a_{\eta_s}^{-1}\tau$ were markedly non-exponential, with the data for (c) with $\theta = 45$ and 60° and (b) with $\theta = 90$° being relatively close and exhibiting the least non-exponential behaviour. In general, the non-exponential character of $g^{(2)}(\tau, q)$ increases with decreasing t_{cent}, T_{LS} and θ. Thus, the scattering for $\theta = 30$° became less non-exponential as the condition varied in the order (a), (b), (c) and (d), but remained more non-exponential than data for $\theta = 90$° and condition (b). Similar trends were noted at all concentrations studied, as shown by the entries of r_ν and γ_ν in *Table 2*.

In some cases, $g^{(2)}(\tau, q)$ was determined for two positions in the light-scattering cell after centrifugation for 12 h: in the 'normal' position, and from a position near the bottom of the cell. These positions correspond to a radial position r_c for the normal position and $r_c + \Delta$ for the lower position, where $r_c \approx 10$ cm and $\Delta = 1$ cm. As shown in *Table 4*, the principal difference in $g^{(2)}(\tau, q)$ at the two positions for a solution with $w = 2.2$ g kg^{-1} is increased r_ν corresponding to the largest coherence time γ_ν^{-1} (and decreased r_ν for the remainder) at the lower position in comparison with the upper. Similar, but smaller, differences are observed for $g^{(2)}(\tau, q)$ for the two positions for a solution with $w = 0.19$ g kg^{-1}.

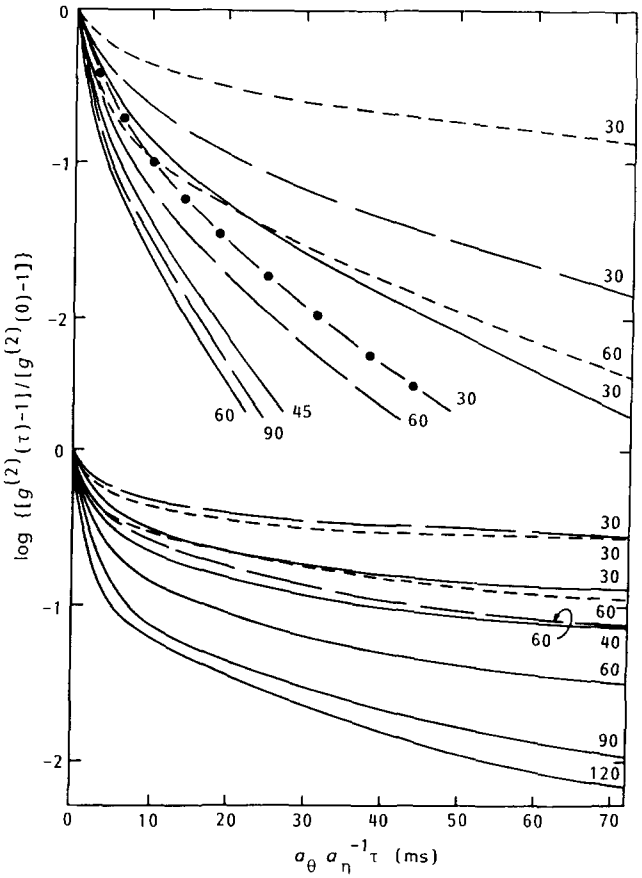

Figure 8 Plots of $\log\{[g^{(2)}(\tau, q) - 1]/[g^{(2)}(0, q) - 1]\}$ *versus* $a_\theta a_\eta^{-1}\tau$/ms for solutions of 0.62 N NaCl with w/g kg^{-1} equal to 0.19 (upper) or 2.2 (lower). The curves represent data with t_{cent} equal to 0.5 h and T_{LS} equal 25°C (·····) and 78°C (——) or t_{cent} equal to 12 h and T_{LS} equal to 25°C (——) and 78°C (— · —)

Table 2 Parameters used in equation (24) to fit the photon-count correlation function[a]

w (g kg^{-1})	T_{LS} (K)	θ (deg)	$a_\theta a_{\eta s}^{-1}\gamma_v^{-1}$ (ms)[b] and $[r_v]$				$R_{H,app}$ (nm)
2.20	298	30	820 [0.55]	16 [0.20]	2.4 [0.19]	0.2 [0.06]	42.3
	351	30	625 [0.56]	28 [0.17]	4.7 [0.18]	0.5 [0.09]	73.7
	298	60	698 [0.36]	21 [0.29]	1.5 [0.39]		60.6
	351	60	679 [0.29]	21 [0.36]	1.5 [0.35]		66.1
1.30	298	30	305 [0.47]	18 [0.34]	2.5 [0.14]	0.5 [0.05]	94
	353	30	180 [0.52]	11 [0.30]	1.9 [0.16]	0.2 [0.02]	77
	298	60	436 [0.23]	30 [0.29]	4.9 [0.48]		154
	353	60	260 [0.19]	32 [0.24]	5.2 [0.57]		141
	298	90	89 [0.26]	11 [0.43]	1.6 [0.31]		70.4
	353	90	89 [0.25]	9.5 [0.44]	1.9 [0.31]		78.2
0.61	298	30	312 [0.39]	13 [0.34]	2.8 [0.22]		157
	353	30	127 [0.43]	7.9 [0.33]	1.8 [0.24]		93.0
	298	60	140 [0.23]	7.5 [0.40]	1.3 [0.37]		48.8
	353	60	117 [0.22]	7.1 [0.27]	1.4 [0.51]		41.7
	298	90	55 [0.22]	4.2 [0.40]	1.1 [0.38]		37.4
	353	90	55 [0.22]	4.2 [0.40]	1.1 [0.38]		37.4
0.19	298	30	241 [0.50]	16 [0.32]	2.3 [0.18]		165
	349	30	53 [0.50]	6.3 [0.40]	0.65 [0.10]		73.2
	298	60	48 [0.29]	8.6 [0.28]	1.8 [0.43]		59.8
	349	60	21 [0.34]	3.7 [0.53]	0.55 [0.13]		42.0
	298	90	11 [0.42]	1.7 [0.52]	0.10 [0.06]		17.6
	349	90	11 [0.42]	1.7 [0.52]	0.10 [0.06]		17.6

[a] All data for $t_{cent}=0.5$ h
[b] a_θ and $a_{\eta_s}^{-1}$ are given by equations (26) and (27), respectively, for $\theta_R=30°$ and $T_g=25°C$

Table 3 Parameters used in equation (24) to fit the photon-count correlation function[a]

t_{cent} (h)	T_{LS} (K)	$a_{\theta_{\eta s}}^{-1}\gamma_v^{-1}$ (ms)[b] and $[r_v]$				$R_{H,app}$ (nm)
0.5	298	134 [0.44]	17 [0.34]	2.5 [0.21]	0.23 [0.01]	110
	312[c]	127 [0.40]	20 [0.31]	3.6 [0.28]	0.27 [0.01]	124
	335[c]	109 [0.41]	11 [0.43]	1.7 [0.16]		122
	352[c]	60 [0.39]	9.7 [0.39]	2.0 [0.22]		106
12	298	36 [0.35]	5.5 [0.44]	1.9 [0.18]	0.2 [0.03]	50
(agitated)	298	386 [0.44]	31 [0.13]	8.5 [0.36]	0.6 [0.07]	101
12	298	36 [0.36]	7.8 [0.33]	1.80 [0.32]		75
	349	24.5 [0.36]	6.2 [0.35]	3.1 [0.26]	0.24 [0.027]	61

[a] All data for $\theta=30°$ and $w=0.19$ g kg^{-1}
[b] a_θ and $a_{\eta_s}^{-1}$ as in *Table 2*
[c] T_{LS} increased from next lowest value, without additional centrifugation

As remarked above, the viscometric data obtained with a low shear stress ($\sigma \lesssim 0.3$ dyn cm^{-2}) for heat-treated sonicated and filtered solutions with $w \leqslant 1.3$ g kg^{-1} did not suggest yield stress behaviour. That is, the materials were liquid and not solid even at the low σ used. Thus, they do not form a macroscopic gel. Nevertheless, the data on $g^{(2)}(\tau, q)$ suggest the presence of supramolecular structures, which can be removed in part through centrifugation. Such structures could contribute to $g^{(2)}(\tau, q)$ as rigid objects (slowly) diffusing in the viscous medium of the solution, or they could contribute through internal scattering from within a gel-like domain (see below).

DISCUSSION

Dilute-solution parameters

The conformation of xanthan in dilute solution has received considerable attention[8,16–34]. It is believed to depend on several parameters, including the ionic strength of the solvent[18,29,32], the temperature[16–18,21,26] and the extent of the pyruvate substitution (64% for the polymer used here)[19,26]. Light-scattering measurements of the (light-scattering-averaged) root-mean-square radius of gyration $R_{g,LS}$, the weight-average molecular weight M_w and the (light-scattering-averaged) hydrodynamic radius $R_{H,LS}$ have been reported on xanthan and products derived therefrom by ultrasonic degradation or chemical modification (e.g. removal of pyruvate groups)[16,17,19–21,31,34]. Studies of $[\eta]$ as a function of M_w have also been reported[8,16–18,22,25,30]. The value $[\eta]=11\,300$ ml g^{-1} reported here for a solution of the 'native' xanthan in 0.62 N NaCl at 25°C is consistent with published values[8,30,31,34]. The experimental data have been interpreted in terms of a two-stranded structure (probably a dimer of two single molecules), with a mass per unit length M_L of 2000 nm^{-1} (refs. 16–18, 21, 22, 24–26 and 30), and a molecular weight of (2 to 6) $\times 10^6$ for the native polymer[19]. The results on $R_{g,LS}$ and $R_{H,LS}$ have been analysed in terms of the persistence length ρ that appears in the worm-like model for polymer conformations[35] to give $\rho \approx 120$ nm (refs 16–19).

For aqueous solutions of xanthan with low concentration of supporting electrolyte, $[\eta]$ is not a

Table 4 Parameters used in equation (24) to fit the photon-count correlation function[a]

w (g kg^{-1})	t_{cent} (h)	θ (deg)	Position[c]	$a_\theta a_{\eta_s}^{-1}\gamma_v^{-1}$ (ms)[b] and $[r_v]$			$R_{H,app}$ (nm)
2.2	0.5	30	C	820 [0.55]	16 [0.20]	2.4 [0.19]	0.2 [0.06]	42
	0.5	60	C	698 [0.36]	21 [0.29]	1.5 [0.39]		61
	12	30	L	729 [0.44]	22 [0.27]	2.1 [0.26]	0.25 [0.03]	65
	12	45	L	698 [0.41]	22 [0.24]	2.2 [0.31]	0.25 [0.04]	53
	12	60	L	771 [0.29]	23 [0.29]	2.1 [0.39]	0.25 [0.03]	52
	12	90	L	729 [0.20]	26 [0.29]	3.1 [0.39]	0.45 [0.12]	41
	12	120	L	729 [0.15]	25 [0.27]	2.3 [0.47]	0.40 [0.11]	34
	12	30	C	729 [0.37]	22 [0.28]	2.8 [0.32]	0.35 [0.03]	79
	12	45	C	729 [0.28]	24 [0.27]	2.4 [0.41]	0.27 [0.04]	50
	12	60	C	729 [0.18]	21 [0.31]	2.1 [0.43]	0.25 [0.08]	31
	12	90	C	729 [0.09]	27 [0.25]	2.4 [0.57]	0.25 [0.10]	26
	12	120	C	729 [0.07]	25 [0.26]	1.6 [0.61]	0.15 [0.06]	21
0.19	0.5	30	C	241 [0.50]	16 [0.32]	2.3 [0.18]		165
	0.5	60	C	48 [0.29]	8.6 [0.28]	1.8 [0.43]		60
	0.5	90	C	11 [0.42]	1.7 [0.52]	0.10 [0.06]		18
	12	30	L	14 [0.56]	2.7 [0.40]	0.25 [0.04]		48
	12	45	L	13 [0.44]	2.2 [0.48]	0.25 [0.08]		29
	12	60	L	12 [0.29]	2.1 [0.66]	0.25 [0.05]		31
	12	30	C	21 [0.49]	2.9 [0.49]	0.28 [0.07]		38
	12	45	C	12 [0.45]	2.0 [0.49]	0.30 [0.06]		31
	12	60	C	11 [0.36]	1.8 [0.55]	0.15 [0.09]		18

[a] All data for $T_{LS}=25°C$
[b] a_θ and $a_{\eta_s}^{-1}$ as in *Table 2*
[c] C and L denote positions near the centre and the bottom of the light-scattering cell, respectively

monotone decreasing function of T, but $\partial[\eta]/\partial T$ may be positive over a range of T centred about some temperature T_M (refs. 17 and 29). Moreover, similar behaviour is observed in a number of other properties, such as the optical rotation[23,26,27,29,32,33,36,37], the intensity of the ^{1}H n.m.r. absorptions associated with the pyruvate and acetate groups on the tripyranose side groups[26] and the viscosity of moderately concentrated solutions[38,39]. In general, T_M increases with the ionic strength of the solvent and the molecular weight of the xanthan. This behaviour has been associated with some structural rearrangements within the helicoidal double-stranded xanthan structure[17]. Since T_M is far in excess of 70°C for solutions in aqueous 0.6 N NaCl[17,27,29], the monotone decrease of η_{sp} with increasing T observed here is not unexpected. The negative $\partial[\eta]/\partial T$ deduced above must be attributed to less drastic structural rearrangements than those involved at T_M. The decrease in $[\eta]$ observed with increasing T for xanthan in aqueous 0.62 N NaCl solution, with $\partial \ln[\eta]/\partial T = -0.0113\ K^{-1}$, is similar to the behaviour observed with a number of chains with a backbone comprising pyranose moieties[40]. In these cases, $\partial \ln[\eta]/\partial T$ may be interpreted in terms of the variation of ρ with T since excluded-volume effects on R_g are normally small for xanthan under the conditions used here (owing to the large ρ), so that:

$$\frac{\partial \ln[\eta]}{\partial T} = \frac{\partial \ln[\eta]}{\partial \ln \rho}\frac{\partial \ln \rho}{\partial T} \tag{28}$$

The factor $\partial \ln[\eta]/\partial \ln \rho$ appearing in equation (28) may be estimated by use of the worm-like model for a chain with persistence length ρ and contour length $L = M/M_L$. For this model, with a polymer heterodisperse in molecular weight, the intrinsic viscosity may be expressed as:

$$[\eta] = \sum w_v [\eta]_v \tag{29}$$

$$M_L[\eta]_v = \pi K_v N_A R_{g,v}^2 R_{H,v}/L_v \tag{30}$$

$$R_{g,v}^2 = (L_v\rho/3)S(L_v/\rho) \tag{31}$$

$$R_{H,v} = (L_v/2)H(L_v/\rho, a/\rho) \tag{32}$$

where w_v is the weight fraction of the chains with intrinsic viscosity $[\eta]_v$ and contour length L_v, a is the diameter of the chain, $S(\ )$ and $H(\ )$ are known functions of the indicated variables[35], and K_v depends on L/ρ but is independent of a/ρ for small a/ρ (ref. 41). Approximate expressions for S, H and K are given by[41]:

$$S(L_v/\rho) \approx (1+4\rho/L_v)^{-1} \tag{33}$$

$$H(L_v/\rho, a/\rho) \approx [(27L_v/16\rho)+\ln^2(3L_v/2a)]^{-1/2} \tag{34}$$

$$K(L_v/\rho) \approx 1+(7/6)\{1+\tanh[0.25\ln(L_v/340\rho)]\} \tag{35}$$

Values of $\partial \ln[\eta]/\partial \ln \rho$ calculated with these relations decrease from 1.5 to 0 as ρ/L_v increases from much less to much greater than unity. For a chain with $\rho \approx 100$ nm and $[\eta]$ in the range observed here, numerical evaluation gives $\partial \ln[\eta]/\partial \ln \rho \approx 1$ for w_v given by a most probable distribution (i.e. $w_v = (L_v/L_n)\exp(-L_v/L_n)$, with L_n the number-average controur length). Thus, with this interpretation, $\partial \ln \rho/\partial T \approx -0.0113\ K^{-1}$ for xanthan, and ρ would decrease from 120 nm at 25°C to 70 nm at 70°C.

In the limit of infinite dilution, the first cumulant K_1 defined as[12,42]:

$$K_1 = -\tfrac{1}{2}\lim_{\tau=0}[\partial \ln g^{(2)}(\tau, g) - 1]/\partial\tau \tag{36}$$

may be interpreted in terms of a hydrodynamic radius:

$$R_{H,LS} = kTq^2/6\pi\eta_s K_1 \tag{37}$$

If $g^{(2)}(\tau, q)$ is represented by equation (24), then:

$$K_1 = \sum r_v\gamma_v \tag{38}$$

Making use of equation (38) with $r_v \approx w_v M_v/M_w$, $R_{H,LS}$ is given by

$$R_{H,LS} = M_w/\sum w_v M_v R_{H,v}^{-1} \tag{39a}$$

where

$$R_{H,v} = kTq^2/6\pi\eta_s\gamma_v \quad (39b)$$

With equation (32) for $R_{H,v}$, numerical evaluation of $R_{H,LS}$ gives $\partial \ln R_{H,LS}/\partial \ln \rho \approx 0.22$ for a most probable distribution of L_v. Thus, with $\partial \ln \rho/\partial T \approx -0.0113$, $R_{H,LS}$ is expected to diminish by 13% over the temperature range 25 to 76°C. By comparison, the experimental K_1^{-1} decreased by 21% over the same temperature interval for the sample with $w = 0.19\,g\,kg^{-1}$ centrifuged for 12 h, in reasonable accord with the predicted change in $R_{H,LS}$.

Viscoelastic behaviour ($[\eta]c > 2$)

Intermolecular association and gelation have been frequent subjects of study in moderately concentrated solutions of xanthan[36,37,43–47], and similar effects are found in this study. The viscometric data in *Table 1* show that the heat-treated, sonicated and filtered xanthan solutions with $w \leqslant 1.3\,g\,kg^{-1}$ flow under a low shear stress (e.g. a stress less than 0.05 Pa; see Experimental section). By contrast, a gel was obtained with a solution with $w = 2.2\,g\,kg^{-1}$. The product $[\eta]c$ is often a useful measure of chain overlap in discussion of intermolecular interactions[11,12,48]. However, the parameter $[\eta]c/n$ is more appropriate if the chains exist as n-mer multiples with n chains bound together along their contour (e.g. $n = 2$ for the double-stranded helicoidal structure suggested for xanthan in dilute solution). Thus, if the strands are considered to be dimers at low c, then the range of applicability of equations (10) and (11) is found to be $[\eta]c/2 < 1$ (see *Figure 2*), in reasonable accord with the behaviour often observed[5,48]. The power-law behaviour for the dependence of η_{sp} on w observed for larger w (i.e. $0.2 < w/g\,kg^{-1} \leqslant 0.93$) is more difficult to understand (see *Figure 3*). As shown by the rheological data on a solution with $w = 2.2\,g/kg^{-1}$ prepared without heating or ultrasonic treatment, the system is able to form a gel, showing that substantial interchain association is possible. The light-scattering data are consistent with this, revealing long coherence times in the representation of $g^{(2)}(\tau, q)$ with equation (24). Therefore, it is presumed that the dependence of η_{sp} on T and w is affected by the presence of supramolecular organization in the solution (see below).

The data in *Figure 3* show that η_{sp} increases less rapidly with increasing c than might be expected on the basis of data on a coil-like polymer such as polystyrene. This is unexpected for a worm-like chain with a large persistence length. Thus, for a rod-like chain, η is predicted[49] and found[50] to increase markedly with concentration, especially as c approaches the value c^* required for the formation of a mesophase. Mesophase formation has been reported for (chain-length degraded) xanthan with $M_w = 140\,000$ in salt-free aqueous solutions for $c = 0.035\,g\,ml^{-1}$ (ref. 51), with the comment that $M_w c^*$ is about constant. These data suggest that the native polymer should form a mesophase at the concentrations shown in *Figure 3*, though none was observed here, or in similar studies of the viscosity of native xanthan in salt-free aqueous solution[52]. (Analysis of the viscometric data in the latter study give values of η_{sp} somewhat larger than those reported here, but with a similar power-law behaviour over the range of concentrations studied here[53].) It is known that association of rod-like chains in ordered arrays with the chain axes parallel leads to marked reduction in η (ref. 54), whereas η may be increased if rod-like chains associate in disordered arrays[55]. Consequently, the low value of $\partial \ln \eta_{sp}/\partial \ln c$ may reflect the preferential formation of nearly ordered arrays of the worm-like chains. This association may also prevent formation of a mesophase, even though the value of $M_w c$ suggests that such a phase should be stable, given the report in ref. 51. Increasing disorder in such aggregates could lead to the formation of a network, as has been observed elsewhere[55]. The observation that $\eta'(0)$ for the gel exceeds the extrapolated value of η_0 for the solution at the same w suggests a suppressed degree of parallel association in the gel as compared with the fluid since dissociation of the crosslink loci would be expected to give a fluid with η_0 at least as large as $\eta'(0)$ for the precursor gel. The wide range in the relaxation times (exemplified, for example, by the data on $R_0(t)$ and $J'(\omega)$) suggests that the worm-like chains cannot be bound by rigid crosslink loci. A similar effect reported for gels formed of poly(γ-benzyl L-glutamate) was attributed to orientation relaxation[56]. The properties of such gels, which are not well understood or even much studied, may be important in a number of situations with worm-like chains, including certain gels in the cytoplasm of eucaryotic cells[57].

Elastic light scattering ($[\eta]c > 2$)

The elastic scattering data support the postulate of interchain association. The scattering from a dilute to moderately concentrated solution may be expressed as[12]:

$$\frac{KcM_w}{R(q)} = \frac{1}{P(q,c)} + cQ(q,c)\Gamma(c) \quad (40)$$

where K is equal to $(4\pi^2/N_A\lambda^4)(n\,\partial n/\partial c)^2$ with n the refractive index of the solvent and $\partial n/\partial c$ the refractive index increment. The latter is taken to be $0.141\,ml\,g^{-1}$ (ref. 22). According to results in ref. 25, for data on high-molecular-weight xanthan with $[\eta]c < 2.5$:

$$1 + c\Gamma(c) \approx (1 + \Gamma_{2,LS}c)^2 \quad (41)$$

where $\Gamma_{2,LS}/[\eta] \approx 0.25$. Moreover, it appears[58] that $Q(q,c) \approx 1$. For high-molecular-weight rod-like chains[12,59]:

$$\lim_{R_g q \gg 1} qR(q)/Kc = \pi M_L \quad (42)$$

As seen in *Figure 7*, plots of $qR(q)/c$ appear to approach an asymptotic limit, as expected with equation (42) for a rod-like chain, giving $M_L = 5000\,nm^{-1}$ for the solution with $w = 0.19\,g\,kg^{-1}$. By comparison, $M_L \approx 2000\,nm^{-1}$ for the xanthan dimer[19,21,24–27], so the observed M_L is consistent with the association suggested above. Moreover, as shown in *Figure 9*, values of $c/R(0)$ obtained here are considerably below values reported[58] for xanthan solution heated to 160°C (under pressure) prior to scattering studies. The deviation between the two sets of data suggests the average aggregate contains about four of the basic dimer structures. The angular dependence at small q also suggests the presence of aggregates in that $qR(q)$ increases with decreasing q over the range studied, whereas in this range $qR(q)$ decreases with decreasing q for similar xanthan solutions heated to 160°C prior to the scattering studies[58]. Thus, unlike the results reported for xanthan solution heated to 160°C, the

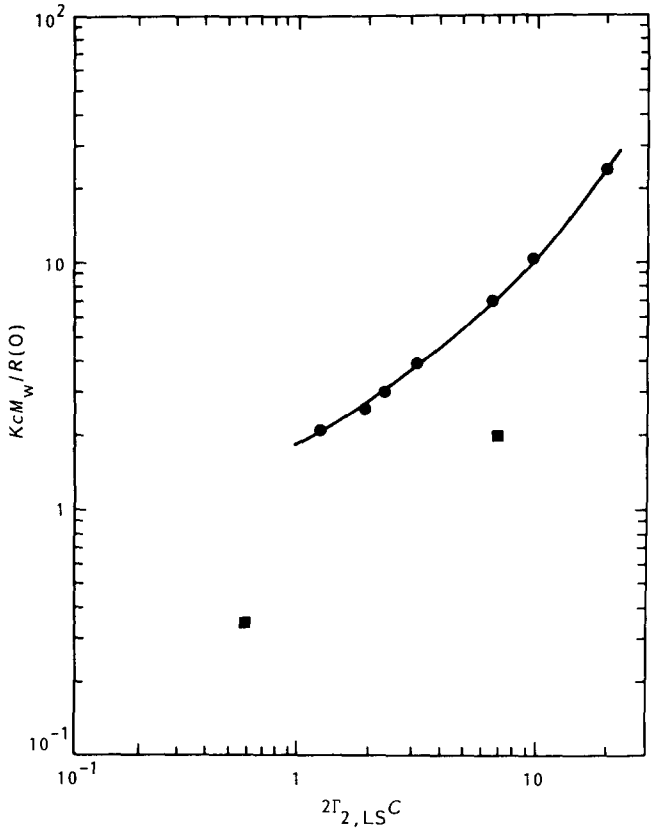

Figure 9 A plot of $KcM_M/R(0)$ *versus* $2\Gamma_{2,LS}c$ for solutions of xanthan in aqueous NaCl for results obtained here (■) and as reported in ref. 58 (●). In both cases, $\Gamma_{2,LS}w/[\eta]$ is put equal to 1450 ml g^{-1} (ref. 58) and $M_w = 2.94 \times 10^6$ (ref. 19)

elastic light scattering obtained here provides evidence for association in solutions heated only to 80°C.

Quasi-elastic light scattering ($[\eta]c > 2$)

The first cumulant $K_1(c,q)$ determined at each c and q does not represent the limiting K_1 at infinite dilution and $q = 0$. It is convenient to represent $K_1(c,q)$ as an apparent diffusion constant $D_{app}(c,q)$, or an apparent hydrodynamic radius $R_{H,app}$:

$$D_{app}(c,q) = K_1(c,q)/q^2 \quad (43)$$

$$R_{H,app} = kTq^2/6\pi\eta_s K_1(c,q) \quad (44)$$

Values of $R_{H,app}$ are reported in *Tables 2–4*. The behaviour observed after 12 h of centrifugation for the solutions with w/g kg^{-1} equal to 0.19 and 2.2 (*Table 4*) give $R_{H,app}$ that decreases with increasing q. Similar behaviour has been reported[19] for solutions of xanthan heated to 160°C prior to light-scattering studies, for which[19]:

$$R_{H,app} \approx R_{H,LS}/(1 + 0.60\Gamma_{2,LS}c)[1 + (D_\rho/D_T - 1)\mathscr{D}(qL)] \quad (45)$$

where D_T is the translational diffusion constant at infinite dilution, L is the chain contour length, D_ρ is the value of D_T for a rod-like chain with length 2ρ, $\mathscr{D}(0) = 0$, $\mathscr{D}(\infty) = 1$ and $\mathscr{D}(qL) \propto (qL)^2$ for small qL. For the range of qL of interest here, $\mathscr{D}(qL)$ given graphically in ref. 19 may be fitted by:

$$\mathscr{D}(qL) \approx 1 - \exp[-(qL/38)^2] \quad (46)$$

As shown in *Figure 10*, the dependence of $R_{H,app}$ on q observed here for well centrifuged samples is close to that given by these relations. The behaviour is much less systematic for samples not centrifuged for a long time, and is taken to reflect supramolecular structure.

The multi-exponential character of the representation of $g^{(2)}(\tau,q)$ by equation (24) and the sensitivity of $g^{(2)}(\tau,q)$ to temperature, especially at the lower w studied, and to the centrifugation history of the sample (e.g. see *Tables 2* and *3* and *Figure 8*) are also characteristic of aggregated structures. Unlike the non-exponential behaviour reported[58] for xanthan solutions heated to 160°C, the $g^{(2)}(\tau,q)$ obtained here for a given w do not generally reduce to a single curve when plotted against $K_1\tau$ for a range of q. This behaviour implicates the role of supramolecular structures in the multi-exponential nature of $g^{(2)}(\tau,q)$, and shows that these structures may be partially and nearly reversibly disrupted by increased T. Presumably, the same sort of supramolecular organization could give rise to gel formation for the sample with $w = 2.2$ g kg^{-1} or to microgel formation at lower concentration. Several factors may contribute to the multi-exponential behaviour seen in $g^{(2)}(\tau,q)$ including: (1) contributions to the scattering from within large, essentially stationary, gel domains in the scattering volume; (2) contributions caused by diffusion of large supramolecular structures; and (3) the effects of hindered rotation on the diffusion of the worm-like chains (or of aggregates formed therefrom with the chain axes nearly parallel). The first is similar to scattering reported from macroscopic gels[60,61], whereas the second resembles the scattering from particles dispersed in a polymer solution. The third corresponds to effects predicted for moderately concentrated solutions of rod-like chains[62].

The third effect mentioned above leads to a markedly non-exponential $g^{(2)}(\tau,q)$. Thus, for a rod-like chain[62], the largest γ_ν (fastest decay), given by $\gamma_L = D_T q^2/2$, differs significantly from the smallest, given by $\gamma_S = [D_T D_R(c)]^{1/2} q$, where the rotational diffusion constant $D_R(c)$ at concentration c may be expressed in the form[62]:

$$D_R(c) = K_R^2 D_T L^{-2}(dc^*/Lc)^2 f(c/c^*) \quad (47)$$

$$f(x) \approx (1 - Bx)^{-2} \quad (48)$$

with d the rod diameter, B a coefficient close to unity[49,50], c^* a concentration close to that c_M required for the formation of a mesophase[50], and K_R a proportionality

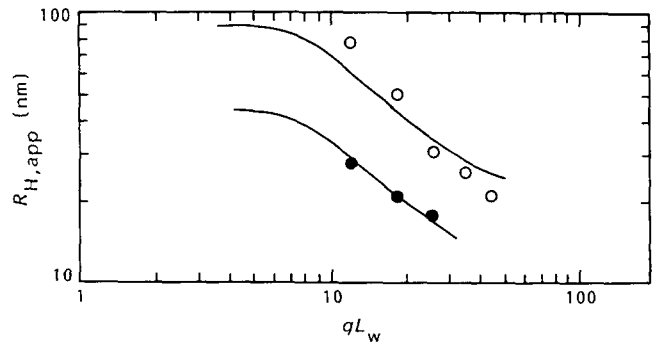

Figure 10 A plot of $R_{H,app}$ *versus* qL_w for solutions of xanthan in aqueous NaCl for w/g kg^{-1} equal to 0.19 (●) and 2.2 (○) (with $L_w = 1610$ nm[19]). The full curves give $kR_{H,app}$ *versus* qL_w from ref. 19, using arbitrary k selected to obtain reasonable coincidence of the curves with the data obtained here

constant ($K_R \approx 100$ (ref. 50)). Thus, for this case:

$$\gamma_S/\gamma_L \approx 2K_R(dc^*/cL)[f(c/c^*)]^{1/2}(qL)^{-1} \quad (49)$$

With neglect of $f^{1/2}$, γ_S/γ_L may be expressed in the form:

$$\gamma_S/\gamma_L \approx (\pi K_R/6)(R_H/L)([\eta]c)^{-1}(qL)^{-1} \quad (50)$$

which might find use for worm-like chains. According to these expressions, curves of $g^{(2)}(\tau, q)$ *versus* $q^2\tau$ are not expected to superpose for all q (i.e. $\gamma_S/\gamma_L \propto q^{-1}$), and γ_S/γ_L decreases with increasing c. The non-exponential decay of $g^{(2)}(\tau, q)$ and the latter features are in qualitative accord with the results found here. With use of equation (32), $R_H/L \approx 0.1$ for a worm-like chain with a persistence length of 100 nm and $L = 10^3$ nm. Accordingly, $\gamma_S/\gamma_L \approx 0.02$ for $\theta = 30°$ for $c = 2\,g\,l^{-1}$. The ratio of the smallest and largest γ_v observed is smaller than this value (see *Table 4*). Moreover, $g^{(2)}(\tau, q)$ appears to depend on the time of centrifugation. These factors indicate that the slow modes should be attributed to the presence of gel-like species rather than to the effects of suppressed rotational diffusion of long worm-like chains.

The possibility that the contributions to $g^{(2)}(\tau, q)$ with large γ_v might derive from the scattering from structure within large gel-like particles may be examined by consideration of the mutual diffusion constant $D_{M,v}$ in the form[60,61]:

$$D_{M,v} = [(K_{os} + \tfrac{4}{3}G_e)/\zeta]_v \quad (51)$$

where ζ is a friction coefficient, G_e is the equilibrium shear modulus, and the 'osmotic modulus' is given by:

$$K_{os} = c\,\partial\Pi/\partial c \quad (52)$$

Following the methods given in ref. 60, as shown in the Appendix, use of the Flory–Huggins relation[63] for Π and reasonable expressions for G_e gives:

$$\frac{D_{M,gel}}{D_{M,liq}} = \left(1 + \frac{4rN_c\phi}{xm(K_{os})_{liq}} + \tfrac{3}{2}(r^2 - 1)\right)\frac{\zeta_{liq}}{\zeta_{gel}} \quad (53)$$

for the ratio of D_M for the gel to the value for the fluid prior to gelation, where ϕ and $r\phi$ are the volume fractions of polymer in the material prior to and after gelation, respectively, x is the polymer degree of polymerization prior to gelation, N_c is the number of crosslinks per molecule, m is the functionality of the loci, and ζ_{liq} and ζ_{gel} are the friction coefficients for the material before and after gelation, respectively. Equation (53) differs from similar relations in refs. 60 and 61 because the gel here is presumed to be swollen to equilibrium in a solution with polymer concentration ϕ rather than in pure solvent. Based on behaviour reported in ref. 61, ζ_{gel}/ζ_{liq} is close to unity (see Appendix). If this is correct, then equation (53) indicates that the contributions to $g^{(2)}(\tau, q)$ with large γ_v cannot be attributed to the scattering from within a gel-like structure inasmuch as $D_{M,gel}/D_{M,liq}$ is expected to be of order unity.

The most likely source of the contributions to $g^{(2)}(\tau, q)$ with large γ_v appear to be from the translational diffusion of microgel particles dispersed in a viscoelastic polymer solution. In this case, the smaller γ are conveniently represented in terms of a scaling length ξ defined as:

$$\xi = \frac{kT}{G\pi\eta_s B(c)}q^2\gamma^{-1} \quad (54)$$

where $B(c)$ is a function of the polymer concentration c. If the particles are spherical, then ξ becomes the particle radius. The function $B(c)$ should be unity for small c, and less than η/η_s for any c. For the system studied here, equation (54) can be expressed in the form:

$$\xi/\text{nm} = 18.03a_\theta a_{\eta_s}^{-1}B^{-1}(c)(\gamma^{-1}/\text{ms}) \quad (55)$$

In studies of suspensions of spheres in aqueous solutions of xanthan, it is reported[53] that $B(c) \approx 1$ for $w < 1\,g\,kg^{-1}$ ($[\eta]c < 10$). Similar behaviour has been reported for other systems[64]. For the suspensions of spheres in xanthan solutions, $B(c)$ increased sharply for larger w, but remained smaller than η/η_s, e.g. $B(c) \approx 10$ for $w = 2\,kg\,kg^{-1}$. The largest γ_v^{-1} observed at 25°C and $\theta = 30°$ in this study correspond to $\xi_v B(c)$ ranging from 15000 nm for $w = 2.2\,g\,kg^{-1}$ to 4300 nm for $w = 0.19\,g\,kg^{-1}$. These values are too large to correspond to the physical radii of the particles observed by light scattering, e.g. much larger than $b \approx 150$ nm reported above. The ratio $\xi B(c)/b$, computed with the smallest γ_v and $b \approx 150$ nm, is greater than unity, but much less than η_{rel}. Thus, the microenvironment probed by the postulated gel particles would have a viscosity smaller than that of the bulk.

With the particulate model, the effect of temperature on $g^{(2)}(\tau, q)$ and $R(q)$ may be related to three effects: (1) variation of the particle size; (2) variation of $B(c)$ through effects on the local environment; and (3) variation of $B(c)$ through effects on the coupling of the particle with adjacent chains. As shown in *Figure 8* and *Table 2*, these effects are slight over the temperature range 25 to 78°C for the solution with $w = 2.2\,g\,kg^{-1}$ studied by light scattering after centrifugation for 0.5 h—as discussed above, a similar sample not given the prolonged heating or subjected to ultrasonic treatment formed a gel at 25°C. Even though the effective viscosity $\eta_{eff} = \eta_s B(c)$ appears to be large, the particles can be partially removed on prolonged centrifugation, as shown by the data in *Figure 8* and *Table 3*. As should be expected, centrifugation is more effective with decreasing w, corresponding to the decrease of $B(c)$ towards unity with decreasing w. Experimentally, for the solution with $w = 2.2\,g\,kg^{-1}$, the sedimentation time required to reduce substantially the contribution to $g^{(2)}(\tau, q)$ suggests that the particles move about 1 cm in 12 h, or $v \approx 2 \times 10^{-5}$ cm s^{-1} in a centrifugal field of 7000g. A force balance on a sphere with radius R sedimenting through a solution under a centrifugal field C gives the sedimentation velocity v equal to:

$$v = 2R^2\,\Delta\rho g C/9\eta_{eff} \quad (56)$$

where η_{eff} is the (effective) viscosity of the solution, $\Delta\rho$ is the difference in density of the sphere and the solution, and C is measured in units of g, the acceleration due to gravity. With the estimates $R^2 = (5/3)b^2$ and $\eta_{eff}R = \eta_s\xi B(c)$, use of equation (56) gives $\Delta\rho$ about equal to 0.03 g cm^{-3}, with $b = 150$ nm and $\xi B(c) = 15000$ nm, as found for the solution with $w = 2.2\,g\,kg^{-1}$. The small value of $\Delta\rho$ is consistent with a highly solvated aggregate, but the significance of the exact value of $\Delta\rho$ obtained with the use of equation (56) is questionable owing to the crudity of the model. Nevertheless, the picture that emerges is one with rather loosely formed aggregates having a range of particle size dispersed in a fluid comprising xanthan dissolved as molecular dimers or small aggregates of the latter. These aggregates may be similar in structure to the supramolecular structure responsible for gelation of xanthan solution. The gel

obtained without heating or ultrasonic treatment is unequivocal evidence for the presence of appreciable intermolecular association. If G_e is interpreted with the usual relation for flexible chain polymers, then for N_c crosslink loci per primary chain with molecular weight M prior to gelation[63]:

$$G_e = N_c kT(cN_A/M) \quad (57)$$

where cN_A/M represents the number of independent solute chains prior to gelation. Assuming the latter to be dimers of the free chains, then $G_e/\text{Pa} \approx 0.91N_c$, for the gel with $w = 2.2\ \text{g kg}^{-1}$ or the observed G_e gives $N_c \approx 65$ for that gel. The microgel particles that remain after heating or ultrasonic treatment may represent the residue of regions with larger than average N_c and a higher than average polymer density. Although a definitive conclusion is not possible, based on the behaviour observed for γ_v, it appears probable that the effect of temperature is to reduce the size of gel particle through partial melting, as opposed to effects on $B(c)$.

Even though the light-scattering data on the moderately concentrated solutions are consistent with the presence of microgel particles covering a range of particle sizes, it should not be inferred that these are so numerous as to dominate all properties of the solution at all w. For example, even though microgel particles are suggested by the scattering for the solution with $w = 0.19\ \text{g kg}^{-1}$, the viscometric data appear to be less affected, in that $P(x)$ can be represented by the limiting relation at infinite dilution (see *Figure 2*). Nevertheless, the difference for the larger w studied between the η_{sp} obtained here and the η_{sp} represented by equation (10) with $P(x)$ given by equation (13) may be caused by the presence of the microgel particles revealed by light scattering.

CONCLUSIONS

Viscometric and light-scattering studies on dilute solutions of native xanthan in aqueous 0.62 N NaCl are interpreted in terms of a negative temperature coefficient for the persistence length. In more concentrated solutions, such that $[\eta]c$ exceeds about 2, the light-scattering behaviour indicates the presence of microgel particles over a range of particle dimensions. These have an increasing effect on the viscometric properties with increasing c, and for $[\eta]c \approx 25$, the system may gel, depending on details of the method used to prepare the sample. At the lowest c, the associated structures appear to have the chain axes in a nearly parallel array. With increasing c the structure is less ordered, giving rise to particle-like structures, which may be the precursors giving a gel at higher concentration.

ACKNOWLEDGEMENTS

It is a pleasure to acknowledge partial support for this study from the National Science Foundation, Industry–University Cooperative Research Program, and the Celanese Research Laboratory. The rheological properties on the gel were carried out by Mr V. Sullivan.

APPENDIX

Following methods given in ref. 60, the use of the Flory–Huggins theory[63] to express K_{os} and G_e for a gel gives:

$$K_{os} + \tfrac{4}{3}G_e = RT\left[v_e^*\left(r^{1/3} + \frac{2r}{m}\right)\phi + \frac{2}{V_1}(\tfrac{1}{2} - \chi_g)r^2\phi^2\right] \quad (A1)$$

where m is the functionality of the crosslink loci, ϕ is the volume fraction of polymer in the solution prior to gelation, v_e^* is the number of strands between crosslinks per unit dry volume of the network, r is the ratio of the concentrations after and prior to gelation, and χ_g is a reduced excess free energy of mixing in the gelled solution. The parameter r may be evaluated by equating the chemical potential of the solvent in the gel and solution. For example, with the Flory–Huggins model, for small ϕ:

$$(\tfrac{1}{2} - \chi_g)\phi^2 r^2 - v_e^* V_1 \phi(r^{1/3} - 2r/m) \approx (\tfrac{1}{2} - \chi_s)\phi^2 + \phi/x \quad (A2)$$

where χ_s is a reduced excess free energy of mixing in the solution prior to gelation and x is the polymer degree of polymerization. With the approximation $\chi_g = \chi_s = \chi$, use of equation (A2) in (A1) gives:

$$K_{os} + \tfrac{4}{3}G_e \approx \frac{RT}{V_1}\left[\left(4v_e^* V_1 \frac{r}{m} - \frac{1}{x}\right)\phi + (3r^2 - 1)(\tfrac{1}{2} - \chi)\phi^2\right] \quad (A3)$$

where r, which increases from unity with increasing v_e^*, may be obtained by use of equation (A2). By comparison, for the solution prior to gelation, $G_e = 0$ and use of the Flory–Huggins model to the same approximation gives:

$$K_{os} = \frac{RT}{V_1}\left(\frac{\phi}{x} + 2(\tfrac{1}{2} - \chi)\phi^2\right) \approx \frac{2RT}{V_1}(\tfrac{1}{2} - \chi)\phi^2 \quad (A4)$$

Thus, for large x, to be a reasonable approximation the ratio of $K_{os} + (4/3)G_e$ for the gel to K_{os} for the solution prior to gelation exceeds unity unless $r \ll 1$, which is unlikely in the present case:

$$\frac{(K_{os} + \frac{4}{3}G_e)_{gel}}{(K_{os})_{liq}} \approx 1 + \frac{4rN_c\phi}{xm(K_{os})_{liq}} + 3\frac{(r^2 - 1)}{2} \quad (A5)$$

Studies on model gels formed with linear chains capped with reactive end groups gave ζ_{gel}/ζ_0 of order unity[61], where ζ_0 is the friction coefficient for the linear chain prior to crosslinking and ζ_{gel} is that for the gel. In the present case, the average chain length prior to gel formation is a factor $N_c + 1$ larger than the chain length between crosslinks. An estimate of the dependence of ζ_0 on chain length is required to evaluate ζ_{gel}/ζ_{liq} from the quoted estimate of ζ_{gel}/ζ_0. For linear flexible chains[12,64,65]:

$$\zeta_0 \propto \zeta^0(R_g^3 c/M)^{(3-\sigma)/3(\sigma-1)} \quad (A6)$$

$$\zeta^0 = 6\pi\eta_s R_H c N_A/M \quad (A7)$$

where $\sigma = 3\,\partial \ln R_g/\partial \ln M$. Thus, with $R_g \propto R_H$, ζ_0 is independent of M, and ζ_{gel}/ζ_{liq} is expected to be of order unity.

REFERENCES

1 Lee, C. C., Chu, S. G. and Berry, G. C. *J. Polym. Sci., Polym. Phys. Edn.* 1973, **21**, 1573
2 Berry, G. C. *J. Chem. Phys.* 1967, **46**, 1338
3 Zimm, B. H. and Crothers, D. M. *Proc. Natl. Acad. Sci. (US)* 1962, **48**, 905
4 Berry, G. C., Park, J. O., Meitz, D. W., Birnboim, M. H. and

Plazek, D. J. *J. Polym. Sci., Polym. Phys. Edn.* 1988 in press

5 Hager, B. L. and Berry, G. C. *J. Polym. Sci., Polym. Phys. Edn.* 1982, **20**, 211

6 Lin, Y. C., Beeson, J. J. and Berry, G. C. *J. Polym. Sci., Polym. Phys. Edn.* 1987, **25**, 1981

7 Simha, R. and Utracki, L. *J. Polym. Sci. (A-2)* 1967, **5**, 853

8 Milas, M., Rinaudo, M. and Tinland, B. *Polym. Bull. (Berlin)* 1985, **14**, 157

9 Berry, G. C. and Plazek, D. J. in 'Glass: Science and Technology' (Eds. D. R. Uhlmann and N. J. Kreidl), Academic Press, New York, 1986, Vol. 3, Ch. 6

10 Markovitz, H. in 'American Institute of Physics Vade-Mecum' (Ed. H. L. Anderson), American Institute of Physics, New York, 1981, Ch. 19

11 Hager, B. L., Berry, G. C. and Tsai, H. H. *J. Polym. Sci., Polym. Phys. Edn.* 1987, **25**, 387

12 Berry, G. C. in 'Encyclopedia of Polymer Science and Engineering', Wiley, New York, 1987, Vol. 8, p. 721

13 Einaga, Y. and Berry, G. C. in 'Microdomains in Polymer Solutions' (Ed. P. Dulin), Plenum, New York, 1985, Ch. 11

14 Williams, G. and Watts, D. C. *Trans. Faraday Soc.* 1970, **66**, 80

15 Lindsey, C. R. and Patterson, G. D. *J. Chem. Phys.* 1980, **73**, 3348

16 Zhang, L., Liu, W., Norisuye, T. and Fujita, H. *Biopolymers* 1987, **26**, 333

17 Liu, W., Sato, T., Norisuye, T. and Fujita, H. *Carbohydr. Res.* 1987, **160**, 267

18 Sho, T., Sato, T. and Norisuye, T. *Biophys. Chem.* 1986, **25**, 307

19 Coviello, T., Kajiwara, K., Burchard, W., Dentini, M. and Crescenzi, V. *Macromolecules* 1986, **19**, 2826

20 Schmidt, M., Paradossi, G. and Burchard, W. *Makromol. Chem., Rapid Commun.* 1985, **6**, 767

21 Sato, T., Norisuye, T. and Fujita, H. *Polym. J.* 1985, **17**, 729

22 Sato, T. Ph.D. Thesis, Osaka University, 1985

23 Kitagawa, H., Sato, T., Norisuye, T. and Fujita, H. *Carbohydr. Polym.* 1985, **5**, 407

24 Sato, T., Norisuye, T. and Fujita, H. *Polym. J.* 1984, **16**, 341

25 Sato, T., Norisuye, T. and Fujita, H. *Macromolecules* 1984, **17**, 2696

26 Paradossi, G. and Brant, D. A. *Macromolecules* 1982, **15**, 874

27 Milas, M. and Rinaudo, M. in 'Solution Properties of Polysaccharides' (Ed. D. A. Brant), ACS Symp. Ser. 150, American Chemical Society, Washington, DC, 1981, p. 25

28 Gelman, R. A. and Barth, H. G. *J. Appl. Polym. Sci.* 1981, **26**, 2099

29 Milas, M. and Rinaudo, M. *Carbohydr. Res.* 1979, **76**, 189

30 Holzwarth, G. *Carbohydr. Res.* 1978, **66**, 173

31 Rinaudo, M. and Milas, M. *Biopolymers* 1978, **17**, 2663

32 Morris, E. R., Rees, D. A., Young, G., Walkinshaw, M. D. and Darke, A. *J. Mol. Biol.* 1977, **110**, 1

33 Holzwarth, G. *Biochemistry* 1976, **15**, 4333

34 Dintzis, F. R., Babcock, G. E. and Tobin, R. *Carbohydr. Res.* 1970, **13**, 257

35 Yamakawa, H. 'Modern Theory of Polymer Solutions', Harper and Row, New York, 1971

36 Southwick, J. G., McDonnell, M. E., Jamieson, A. M. and Blackwell, J. *Macromolecules* 1979, **12**, 305

37 Morris, V. J., Franklin, D. and I'Anson, K. *Carbohydr. Res.* 1983, **121**, 13

38 Jamieson, A. M., Southwick, J. G. and Blackwell, J. *Faraday Symp. Chem. Soc.* 1983, **18**, 131

39 Jeanes, A., Pittsley, J. E. and Senti, F. R. *J. Appl. Polym. Sci.* 1961, **5**, 519

40 Kurata, M. and Stockmayer, W. H. *Adv. Polym. Sci.* 1963, **3**, 196

41 Berry, G. C. *J. Polym. Sci., Polym. Phys. Edn.* 1988, **26**, 1137

42 Berne, B. J. and Pecora, R. 'Dynamic Light Scattering', Wiley-Interscience, New York, 1976

43 Lim, T., Uhl, J. T. and Prud'homme, R. K. *J. Rheol.* 1984, **28**, 367

44 Ross-Murphy, S. B., Morris, V. J. and Morris, E. R. *Faraday Symp. Chem. Soc.* 1983, **18**, 115

45 Southwick, J. G., Jamieson, A. M. and Blackwell, J. *J. Appl. Polym. Sci., Appl. Polym. Symp.* 1983, **37**, 385

46 Smith, J. H., Symes, K. C., Lawson, C. J. and Morris, E. R. *Int. J. Biol. Macromol.* 1981, **3**, 129

47 Southwick,, J. G., Lee, H., Jamieson, A. M. and Blackwell, J. *Carbohydr. Res.* 1980, **84**, 287

48 Graessley, W. W. *Adv. Polym. Sci.* 1974, **16**, 1

49 Doi, M. *J. Phys. (Paris)* 1975, **36**, 607

50 Venkatraman, S., Berry, G. C. and Einaga, Y. *J. Polym. Sci., Polym. Phys. Edn.* 1985, **23**, 1275

51 Maret, G., Milas, M. and Rinaudo, M. *Polym. Bull. (Berlin)* 1981, **4**, 291

52 Whitcomb, P. J. and Macosko, C. M. *J. Rheol.* 1978, **22**, 493

53 Jamieson, A. M., Southwick, J. G. and Blackwell, J. *J. Polym. Sci., Polym. Phys. Edn.* 1982, **20**, 1513

54 Chu, S. G., Venkatraman, S., Berry, G. C. and Einaga, Y. *Macromolecules* 1981, **14**, 939

55 Wong, C. P. and Berry, G. C. *Polymer* 1979, **20**, 229

56 Murthy, A. K. and Muthukumar, M. *Macromolecules* 1987, **20**, 564

57 Nossal, R. in 'Reversible Gelation in Polymers' (Ed. P. S. Russo), ACS Symp. Ser. 350, American Chemical Society, Washington DC, 1987

58 Coviello, T., Burchard, W., Dentini, M. and Crescenzi, V. *Macromolecules* 1987, **20**, 1102

59 Casassa, E. F. *J. Chem. Phys.* 1955, **23**, 596

60 Tanaka, T., Ishiwata, S. and Ishimoto, C. *Phys. Rev. Lett.* 1977, **38**, 771

61 Munch, J. P., Candau, S., Duplessix, R., Picot, C., Herz, J. and Benoit, H. *J. Polym. Sci., Polym. Phys. Edn.* 1976, **14**, 1097

62 Doi, M. and Edwards, S. F. *J. Chem. Soc., Faraday Trans. II* 1978, **74**, 560

63 Flory, P. J. 'Principles of Polymer Chemistry', Cornell University Press, Ithaca, NY, 1953

64 de Gennes, P. G. 'Scaling Concepts in Polymer Physics', Cornell University Press, Ithaca, NY, 1979

65 Adam, M. and Delsanti, M. *Macromolecules* 1985, **18**, 1760